Organic Electronics 13 (2012) 2647–2652

Contents lists available at SciVerse ScienceDirect

Organic Electronics

journal homepage: www.elsevier.com/locate/orgel

Inverted photovoltaic cells of nanocolumnar C_{60} filled with solution processed small molecule 3-Q

M. Thomas [a,b,*], W. Li [b], Z.S. Bo [c], M.J. Brett [a,b]

[a] Department of Electrical and Computer Engineering, University of Alberta, Edmonton, AB, Canada T6G 2V4
[b] NRC National Institute for Nanotechnology, Edmonton, AB, Canada T6G 2M9
[c] College of Chemistry, Beijing Normal University, Beijing 100875, China

ARTICLE INFO

Article history:
Received 10 May 2012
Received in revised form 21 July 2012
Accepted 28 July 2012
Available online 9 August 2012

Keywords:
Glancing angle deposition
Small molecule thin films
Organic solar cells
C_{60} fullerene
Nanostructure
Inverted architecture

ABSTRACT

Nanocolumnar C_{60} films for inverted organic photovoltaic cells (OPVs) were fabricated by glancing angle deposition (GLAD), and morphologies depending on variation in deposition angle were studied. To complete the OPV devices, small molecules of the donor material 3-Q were spin coated into the C_{60} films. In order to avoid the difficulties of solvent stability of the C_{60} films, acetone was used as the process solvent for spin coating. The nanocolumnar morphology improves exciton harvesting by increasing absorbance while providing an effective conductive path for charge carriers. The resulting GLAD C_{60}/3-Q devices outperformed both planar devices and $PC_{61}BM$:3-Q bulk heterojunctions with threefold and twofold short-circuit current increases, respectively.

1. Introduction

Organic photovoltaic cells (OPVs) are suitable candidates for low-cost solar power generation [1–13]. State of the art architectures are solution-processed polymer blends or so-called bulk heterojunctions [2–4,6–10,12,13]. Small molecules, however, allow for better morphology control [14,15] and several fabrication approaches can be used, such as thermal evaporation [16], organic phase vapor deposition [17,18], solution-processed blending [19,20], blending through co-deposition [21–23], and glancing angle deposition [24–29].

OPVs are limited by the exciton diffusion length in the active layer materials, and in order to improve performance morphology control is critical. The photoactive layer in bulk heterojunctions is typically disordered exhibiting pocket domains and dead-ends which can limit charge transport and thus overall device performance [21,30,31]. In contrast, the fabrication process in this work utilizes glancing angle deposition (GLAD) which employs substrate rotation at oblique flux incidence in order to fabricate porous films [32,33]. Due to this substrate motion a vertically oriented network of interpenetrating donor and acceptor columns can be deposited which promises to maximize charge transport and minimize trap states resulting from dead-ends [6,34,35].

We previously reported on inverted architecture OPVs based on GLAD C_{60} fullerene films filled with the donor polymer poly[3-(4-carboxybutyl)thiophene-2,5-diyl] and showed a twofold increase in short-circuit current compared with bulk heterojunctions [29]. While this GLAD based architecture showed very strong promise for OPV performance improvement, suitable solvent-donor combinations have to be found in order to fully exploit this potential. Thus, a major challenge when filling the C_{60} nanocolumnar structure with the polymer solution through spin coating was that the C_{60} films dissolved in most commonly used solvents such as chloroform or

* Corresponding author at: Department of Electrical and Computer Engineering, University of Alberta, Edmonton, AB, Canada T6G 2V4. Tel.: +1 780 492 7926; fax: +1 780 492 2863.
E-mail address: mike.thomas@ualberta.ca (M. Thomas).

1566-1199/$ - see front matter © 2012 Elsevier B.V. All rights reserved.
http://dx.doi.org/10.1016/j.orgel.2012.07.039

dichlorobenzene. We were required to use dimethyl-sulfoxide as solvent which limited the choice of donor materials we could use and resulted in poor donor filling of our nanocolumnar C_{60} structures.

In this work, we fabricate devices with an active layer made entirely from small molecules and thus demonstrate a processing route which can be used together with GLAD fabricated nanocolumnar C_{60} films (see Fig. 1). The star molecule 3-Q (4,4′,4″,4‴-(5,5′,5″,5‴-([2,1,3]benzothiadiazole-4,5,6,7-tetrayl)tetrakis(3-hexylthiophene-5,2-diyl))tetrakis(*N*,*N*-diphenylaniline)) [36] is soluble in acetone which is a strong advantage when working with C_{60} fullerene films since acetone does not dissolve the C_{60} and thus does not adversely affect the GLAD nanocolumnar morphology. We use spin coating of 3-Q into the GLAD C_{60} films and investigate the filling properties and effect on device performance.

2. Experimental

2.1. Thin film deposition

Using thermal evaporation, C_{60} fullerene powder (Sigma Aldrich, 99.9% pure) was deposited on indium tin oxide (ITO) coated glass substrates (Delta Technologies, ITO thickness ~120 nm with sheet resistance ~20 Ω sq^{-1}) where these substrates acted as the cathode of our devices. The ITO coated glass substrates were prepared by sequential sonication in methylene chloride, Millipore water (18 MΩ cm), and 2-propanol for 10 min each. Next the substrates were plasma cleaned for 10 min in an air plasma using a Harrick plasma (PDC 32G, 18 W) cleaner at ~0.1 Torr working pressure. In order to improve electron transparency of the cathode, Cs_2CO_3 was implemented as an interfacial modifier. This Cs_2CO_3 layer was cast from a 0.2 wt.% solution in 2-ethoxyethanol and annealed at 150 °C for 20 min [37].

The C_{60} powder was stored in inert atmosphere and prior to evaporation the C_{60} powder was kept in an alumina crucible (Delta Glass) in vacuum. In order to purify the C_{60} powder immediately prior to evaporation it was kept at 250 °C in the process chamber for 12 h at a pressure of 1×10^{-7} Torr. During subsequent thermal evaporation the crucible was heated up to 450 °C and the working pressure was about 2×10^{-7} Torr. Using a quartz crystal thickness monitor deposition rates between 0.5 and 1.0 Å s^{-1} were maintained. During the GLAD process the substrate tilt angle α (measured relative to the substrate normal) controls spacing of the C_{60} nanocolumns, and in this work $\alpha = 75°$ and 80° were used to fabricate devices. In addition, planar films at $\alpha = 0°$ were prepared for comparison. During evaporation, substrate rotation was applied to achieve a more homogenous film thickness distribution. Rotation speeds were kept constant relative to the deposition rate and varied from 0.2 to 0.6 rpm.

2.2. Device fabrication

5 mg mL^{-1} of 3-Q were dissolved in acetone (HPLC, Sigma–Aldrich) and in order to improve dissolution the mixture was kept in an ultrasonic bath for about 1 h. The resulting solution was spun directly onto the C_{60} films at 400 rpm for 1 min in air. During this process the pipettes and solution were kept at 50 °C in order to maintain solubility of the 3-Q. For anode fabrication, V_2O_5 (~20 nm) and Al (~120 nm) were thermally evaporated at a rate of 0.01 and 5 Å s^{-1}, respectively. Five devices per substrate with a (0.155 ± 0.008) cm^2 device area were made. For every deposition angle a series of multiple sets of devices were fabricated and analyzed. For comparison, bulk heterojunctions of 3-Q and $PC_{61}BM$ ([6,6]-phenyl C_{61} butyric acid methyl ester) were fabricated as described in [36] with an active layer thickness of 70 nm.

2.3. Characterization techniques

Morphology was analyzed using a Hitachi S-4800 scanning electron microscope (SEM) with a secondary electron detector. Absorbance was measured for C_{60} films only and in C_{60}/3-Q double layers using a Perkin-Elmer NIR-UV Lambda 900 spectrophotometer. All films used for absorbance measurements were deposited on fused silica following the same processes used for device fabrication. *J–V* characteristics were measured using an Oriel 91191 1000 W solar simulator together with a Keithley 2400 source meter. Light intensity was calibrated using a Si solar cell standard (NREL certified) together with a KG-5 filter (PV Measurements Inc., PVM624).

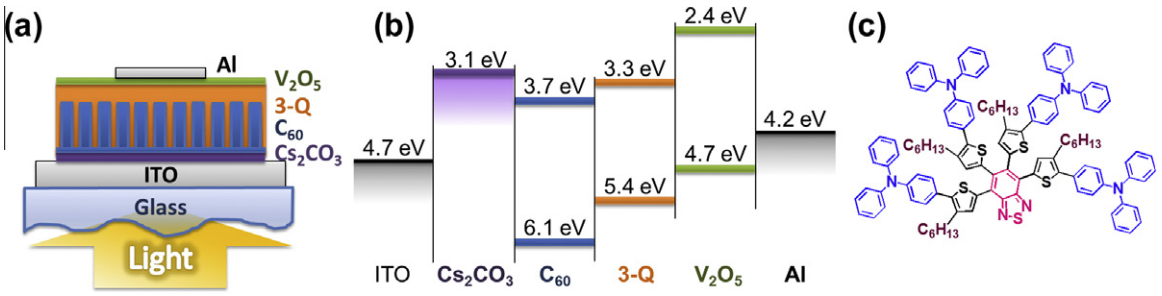

Fig. 1. Device concept: (a) Device architecture with a nanocolumnar C_{60} fullerene film filled with 3-Q donor molecules. (b) Corresponding electronic structure including interfacial layer Cs_2CO_3 and hole transparent layer V_2O_5. (c) 3-Q star molecule.

3. Results and discussion

3.1. Film morphology

Morphology control is central to this work and follows techniques previously reported in detail for fabricating nanocolumnar films [29]. The thicknesses of both morphologies of GLAD C_{60} films are nominally 160 nm. C_{60} average column diameters are (65 ± 10) nm for the $\alpha = 75^\circ$ and (105 ± 10) nm for the $\alpha = 80^\circ$ films, as seen in Fig. 2. Intercolumn spacing is controlled by adjusting the deposition angle α and results from ballistic shadowing of the incoming particle flux during deposition. The average spacing was measured to be (40 ± 20) nm for films deposited at $\alpha = 75^\circ$ and (60 ± 20) nm for $\alpha = 80^\circ$. Intercolumn spacing affects both the filling properties of the spin coated donor and the heterointerface area, and in addition, exciton harvesting can improve when intercolumn spacing more closely matches the exciton diffusion length of the donor which is estimated to be about 10–20 nm. For comparison in Fig. 2, a 30 nm thick planar film is shown, and it is observed that there is some minor surface roughness, perhaps originating from the roughness of the underlying ITO.

3.2. Compatibility of acetone as process solvent

In our previous work we reported that the use of the donor solvent is one of the main limitations for subsequent solution processing of our GLAD structured C_{60} OPVs. The challenge is to find a solvent which does not dissolve the nanostructured C_{60} films while at the same time provides a good filling of donor molecules into the nanocolumnar structures. Since C_{60} fullerenes are highly symmetric molecules and therefore have low polarity, C_{60} films can easily be dissolved in non-polar solvents such as chloroform or chlorobenzene which are commonly used in OPV fabrication [29]. In contrast, acetone is a polar aprotic solvent and nanocolumnar C_{60} is stable when treated with this solvent. Consequently, the choice of solvent limits the applicability of various donors to the device. The commonly used poly(3-hexylthiophene-2,5-diyl) (P3HT) dissolves in some non-polar solvents, however it does not dissolve in acetone. In contrast, 3-Q does dissolve in acetone and therefore can be used for spin coating on nanocolumnar C_{60}.

Fig. 3 shows the GLAD structured C_{60} films after spin coating with 3-Q dissolved in acetone. Compared with previous results [29], a good infiltration of 3-Q into the nanocolumnar structures is observed. In particular, a previously observed drawback using dimethyl-sulfoxide (DMSO) as solvent were voids and empty pockets after spin coating [29]. Contact angle measurements of DMSO and acetone on a planar C_{60} film were performed. For DMSO a contact angle of (27 ± 3)° was observed. However, acetone instantly wetted the C_{60} surface and no contact angle could be measured. Hence, due to the lower polarity of acetone, filling of a donor into nanocolumnar C_{60} films is significantly improved.

3.3. Absorbance

Fig. 4 shows the absorbance of C_{60}/3-Q double layers. For comparison, spectra for a pure 3-Q film and a pure GLAD C_{60} film deposited at $\alpha = 80^\circ$ are included. The pure C_{60} spectrum is in agreement with previously observed results [29], with a C_{60} peak observed at 344 nm. In addition, C_{60} causes the broad peak formation between 400 nm and 500 nm with a local maximum at 450 nm. The mass density of C_{60} films decreases with increasing deposition angles α [38], leading to the decreasing absorption of the C_{60} peaks when going from $\alpha = 75^\circ$ to 80°. The 3-Q absorbance spectrum has two broader regions, one at around 515 nm, which is comparable with the absorption in P3HT, and one at lower wavelengths of around 350 nm which provides additional sensitivity in the ultraviolet.

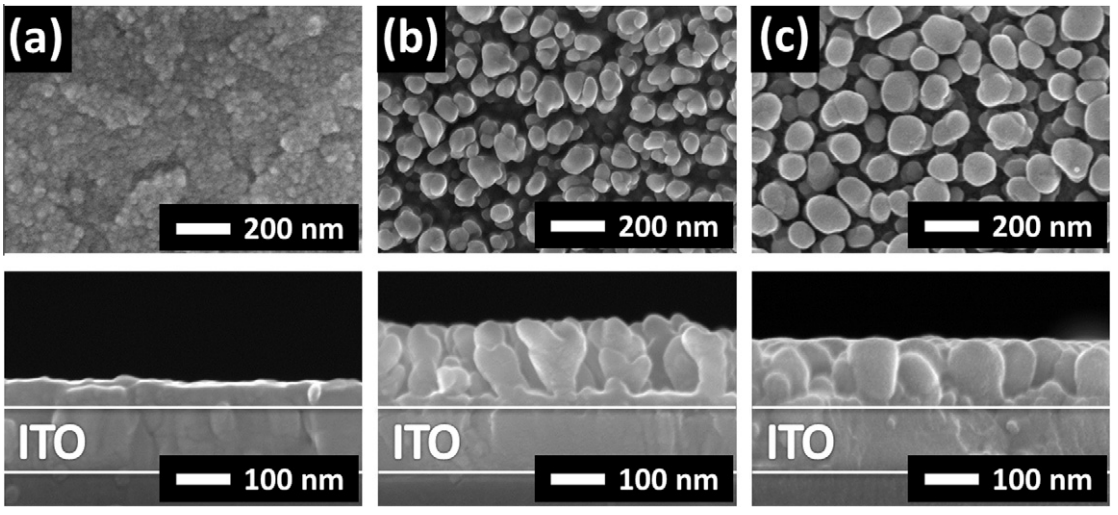

Fig. 2. Scanning electron microscopy images of glancing angle deposited C_{60} fullerene films with top (image above) and side views (image below). (a) Planar C_{60} film. (b) C_{60} film deposited at $\alpha = 75^\circ$. (c) C_{60} film deposited at $\alpha = 80^\circ$. The ITO layer is marked with lines; above is the C_{60} film and below is glass.

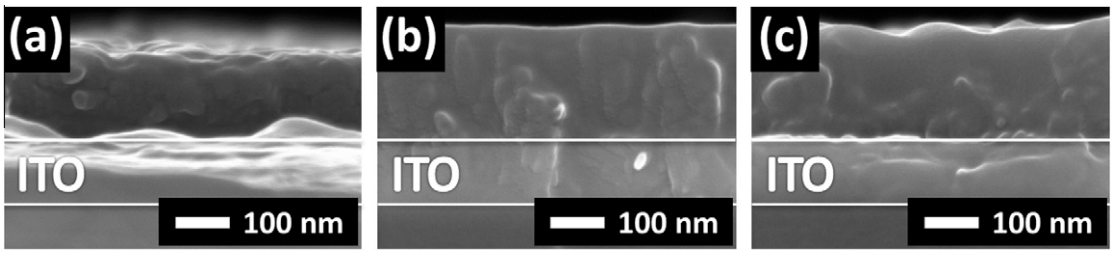

Fig. 3. Scanning electron microscopy images after spin coating of 3-Q onto the C_{60} films. (a) Planar C_{60} film with planar 3-Q film on top. Due to variations in cleaving the substrate the photoactive layer cleaved further back from the edge than the ITO substrate. (b) C_{60} film deposited at $\alpha = 75°$ with infiltrated 3-Q. (c) C_{60} film deposited at $\alpha = 80°$ with infiltrated 3-Q.

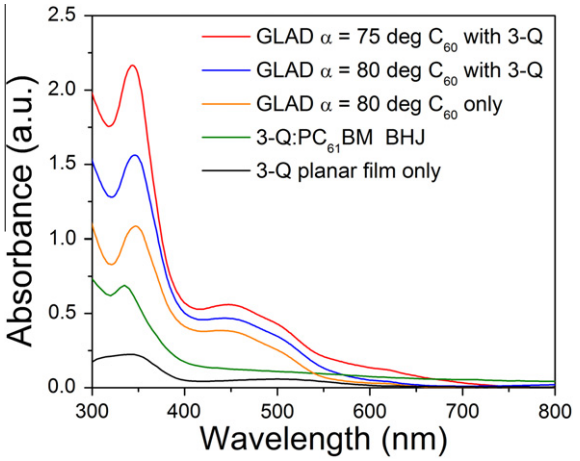

Fig. 4. Absorbance spectra of a GLAD C_{60} films filled with 3-Q. For comparison, a 3-Q:$PC_{61}BM$ bulk heterojunction, a pure GLAD C_{60} film deposited at $\alpha = 80°$ and a pure planar 3-Q film are shown (Vertical order in legend follows vertical sequence of graphs).

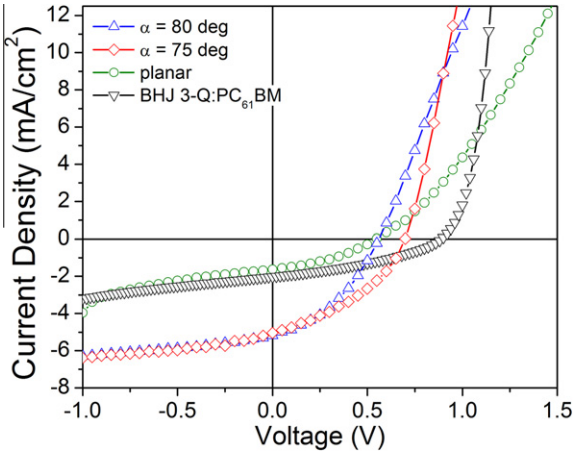

Fig. 5. *J–V* characteristics of GLAD devices compared with a planar device and a bulk heterojunction.

The onset for the 3-Q spectrum appears at ~615 nm indicating an optical band gap of 2.0 eV which is in agreement with previous results [36]. It can be observed that the C_{60}/3-Q double layer peaks are of higher absorption compared with the bulk heterojunction spectrum, due to the lower thickness of the bulk heterojunction's active layer.

3.4. Device performance

J–V characteristics of the fabricated devices were measured and are shown in Fig. 5 where GLAD device performance is compared to bulk heterojunction and planar devices. The open circuit voltage is lower in GLAD devices compared with the bulk heterojunction, as previously reported [29], and can be attributed to oxygen exposure during device fabrication. However, the short-circuit current is significantly increased in the GLAD devices and has doubled compared with the bulk heterojunction.

Table 1 shows the average device parameters for each device series. Both GLAD devices perform similarly within error ranges. The slope of the *J–V* curve for the $\alpha = 80°$ device at $J = 0$ mA cm^{-2} is lower compared with the $\alpha = 75°$ device. This behavior could be attributed to a higher series resistance which also leads to a slight variation in V_{OC} between both GLAD devices. The highest power conversion efficiency (PCE) is observed for the GLAD devices fabricated at $\alpha = 75°$. This PCE is a twofold improvement over the bulk heterojunction and a threefold improvement relative to the planar device.

4. Conclusions

Organic photovoltaic devices based on glancing angle deposited C_{60} fullerene films filled with donor 3-Q small molecules have been fabricated and characterized. The use of acetone significantly improved donor filling compared with previously reported devices which used dimethyl-sulfoxide as process solvent for poly[3-(4-carboxybutyl)thiophene-2,5-diyl]. In addition, the morphology of the nanocolumnar C_{60} fullerene films was preserved when using acetone. The resulting nanocolumnar devices were compared with a bulk heterojunction and a twofold increase in power conversion efficiency of GLAD fabricated devices was observed. The GLAD nanocolumnar morphology allows thicker devices and thus increased absorbance compared with bulk heterojunctions while enabling an effective conductive path for charge carriers.

The fabrication process using acetone and a small molecule donor provides a route to improved performance in inverted OPVs utilizing C_{60} in a nanocolumnar architecture.

Table 1
Performance parameters for fabricated device series. All thermally evaporated devices have the following architecture: glass/ITO/Cs_2CO_3/active materials/V_2O_5/Al. For comparison, the values for a 3-Q:$PC_{61}BM$ heterojunction are added.

Active materials	J_{SC} (mA cm^{-2})	V_{OC} (V)	PCE (%)	FF	Best PCE (%)
C_{60} ($\alpha = 80°$), 3-Q	4.7 ± 0.3	0.5 ± 0.1	0.8 ± 0.3	0.34 ± 0.05	1.3
C_{60} ($\alpha = 75°$), 3-Q	4.1 ± 0.5	0.7 ± 0.1	1.0 ± 0.2	0.33 ± 0.03	1.4
Planar C_{60}, 3-Q	1.3 ± 0.3	0.6 ± 0.1	0.3 ± 0.1	0.38 ± 0.05	0.5
3-Q:$PC_{61}BM$	2.0 ± 0.1	0.9 ± 0.1	0.7 ± 0.1	0.38 ± 0.01	0.8

With our previous work [29] and in this article we have shown a twofold short-circuit current increase due to our GLAD structured morphology compared with bulk heterojunctions in two different material systems, one utilizing a conjugated polymer P3CBT, the other using a small molecule 3-Q. This is a strong indication that this architecture would be able to achieve superior performance compared with state-of-the-art bulk heterojunctions if an appropriate solvent-donor combination can be found which can complement the C_{60} nanocolumnar structure.

Acknowledgments

The authors would like to thank Tate C. Hauger for device fabrication and performance measurements, Dr. Erik Luber for contact angle measurements, Dr. Jonathan Veinot for access to the top electrode evaporator, and Brian J. Worfolk for discussion. In addition, we gratefully acknowledge the support of the following organizations: Vanier Canada Graduate Scholarships Program, NRC National Institute for Nanotechnology, Natural Sciences and Engineering Research Council of Canada (NSERC), Killam Trusts, Alberta Innovates: Technology Futures (AITF), the School of Engineering and Environment (SEE) at the University of Alberta, the Canada Research Chairs Program, and Micralyne, Inc.

References

[1] C.W. Tang, Two-layer organic photovoltaic cell, Appl. Phys. Lett. 48 (1986) 183–185.
[2] N.S. Sariciftci, L. Smilowitz, A.J. Heeger, F. Wudl, Photoinduced electron transfer from a conducting polymer to buckminsterfullerene, Science 258 (1992) 1474–1476.
[3] J.J.M. Halls, C.A. Walsh, N.C. Greenham, E.A. Marseglia, R.H. Friend, S.C. Moratti, A.B. Holmes, Efficient photodiodes from interpenetrating polymer networks, Nature 376 (1995) 498–500.
[4] S.E. Shaheen, R. Radspinner, N. Peyghambarian, G.E. Jabbour, Fabrication of bulk heterojunction plastic solar cells by screen printing, Appl. Phys. Lett. 79 (2001) 2996–2998.
[5] J.G. Xue, S. Uchida, B.P. Rand, S.R. Forrest, Asymmetric tandem organic photovoltaic cells with hybrid planar-mixed molecular heterojunctions, Appl. Phys. Lett. 85 (2004) 5757–5759.
[6] K.M. Coakley, M.D. McGehee, Conjugated polymer photovoltaic cells, Chem. Mater. 16 (2004) 4533–4542.
[7] H. Spanggaard, F.C. Krebs, A brief history of the development of organic and polymeric photovoltaics, Sol. Energy Mater. Sol. Cells 83 (2004) 125–146.
[8] J. Roncali, Linear π-conjugated systems derivatized with C_{60}-fullerene as molecular heterojunctions for organic photovoltaics, Chem. Soc. Rev. 34 (2005) 483–495.
[9] S.E. Gledhill, B. Scott, B.A. Gregg, Organic and nano-structured composite photovoltaics: an overview, J. Mater. Res. 20 (2011) 3167–3179.
[10] P.W.M. Blom, V.D. Mihailetchi, L.J.A. Koster, D.E. Markov, Device physics of polymer: fullerene bulk heterojunction solar cells, Adv. Mater. 19 (2007) 1551–1566.
[11] J.Y. Kim, K. Lee, N.E. Coates, D. Moses, T.-Q. Nguyen, M. Dante, A.J. Heeger, Efficient tandem polymer solar cells fabricated by all-solution processing, Science 317 (2007) 222–225.
[12] B.C. Thompson, J.M.J. Fréchet, Polymer-fullerene composite solar cells, Angew. Chem. Int. Ed. 47 (2008) 58–77.
[13] H.-Y. Chen, J. Hou, S. Zhang, Y. Liang, G. Yang, Y. Yang, L. Yu, Y. Wu, G. Li, Polymer solar cells with enhanced open-circuit voltage and efficiency, Nat. Photonics 3 (2009) 649–653.
[14] P. Peumans, S. Uchida, S.R. Forrest, Efficient bulk heterojunction photovoltaic cells using small-molecular-weight organic thin films, Nature 425 (2003) 158–162.
[15] M. Riede, T. Mueller, W. Tress, R. Schueppel, K. Leo, Small-molecule solar cells – status and perspectives, Nanotechnology 19 (2008) 424001.
[16] S. Pfuetzner, J. Meiss, A. Petrich, M. Riede, K. Leo, Thick C-60:ZnPc bulk heterojunction solar cells with improved performance by film deposition on heated substrates, Appl. Phys. Lett. 94 (2009) 223307.
[17] F. Yang, M. Shtein, S.R. Forrest, Controlled growth of a molecular bulk heterojunction photovoltaic cell, Nat. Mater. 4 (2004) 37–41.
[18] M. Shtein, H.F. Gossenberger, J.B. Benziger, S.R. Forrest, Material transport regimes and mechanisms for growth of molecular organic thin films using low-pressure organic vapor phase deposition, J. Appl. Phys. 89 (2001) 1470–1476.
[19] G. Wei, S. Wang, K. Renshaw, M.E. Thompson, S.R. Forrest, Solution-processed squaraine bulk heterojunction photovoltaic cells, ACS Nano 4 (2010) 1927–1934.
[20] A. Sanchez-Diaz, R. Pacios, U. Munecas, T. Torres, E. Palomares, Charge transfer reactions in near IR absorbing small molecule solution processed organic bulk-heterojunction solar, Org. Electron. 12 (2011) 329–335.
[21] P. Peumans, A. Yakimov, S.R. Forrest, Small molecular weight organic thin-film photodetectors and solar cells, J. Appl. Phys. 93 (2003) 3693–3723.
[22] J.G. Xue, B.P. Rand, S. Uchida, S.R. Forrest, A hybrid planar-mixed molecular heterojunction photovoltaic cell, Adv. Mater. 17 (2005) 66–71.
[23] R. Pandey, R.J. Holmes, Graded donor-acceptor heterojunctions for efficient organic photovoltaic cells, Adv. Mater. 22 (2010) 5301–5305.
[24] J.G. Van Dijken, M.D. Fleischauer, M.J. Brett, in: Morphology Control of CuPc Thin Films using Glancing Angle Deposition, PVSC: 2008 33rd IEEE Photovoltaic Specialists Conference, vols. 1–4, 2008, pp. 1222–1225.
[25] N. Li, S.R. Forrest, Tilted bulk heterojunction organic photovoltaic cells grown by oblique angle deposition, Appl. Phys. Lett. 95 (2009) 123309.
[26] Y. Zheng, R. Bekele, J. Ouyang, J. Xue, Organic photovoltaic cells with vertically aligned crystalline molecular nanorods, Org. Electron. 10 (2009) 1621–1625.
[27] J.G. Van Dijken, M.D. Fleischauer, M.J. Brett, Solvent effects on ZnPc thin films and their role in fabrication of nanostructured organic solar cells, Org. Electron. 12 (2011) 2111–2119.
[28] J.G. Van Dijken, M.D. Fleischauer, M.J. Brett, Controlled nanostructuring of CuPc thin films via glancing angle deposition for idealized organic photovoltaic architectures, J. Mater. Chem. 21 (2011) 1013–1019.
[29] M. Thomas, B.J. Worfolk, D.A. Rider, M.T. Taschuk, J.M. Buriak, M.J. Brett, C_{60} fullerene nanocolumns-polythiophene heterojunctions for inverted organic photovoltaic cells, ACS Appl. Mater. Interf. 3 (2011) 1887–1894.
[30] B.A. Gregg, M.C. Hanna, Comparing organic to inorganic photovoltaic cells: theory, experiment, and simulation, J. Appl. Phys. 93 (2003) 3605–3614.
[31] B.A. Gregg, Excitonic solar cells, J. Phys. Chem. B 107 (2003) 4688–4698.

[32] K. Robbie, M.J. Brett, A. Lakhtakia, Chiral sculptured thin films, Nature 384 (1996) 616.
[33] M.M. Hawkeye, M.J. Brett, Glancing angle deposition: fabrication, properties, and applications of micro- and nanostructured thin films, J. Vac. Sci. Technol. A 25 (2007) 1317–1335.
[34] J.S. Kim, Y. Park, D.Y. Lee, J.H. Lee, J.H. Park, J.K. Kim, K. Cho, Poly(3-hexylthiophene) nanorods with aligned chain orientation for organic photovoltaics, Adv. Funct. Mater. 20 (2010) 540–545.
[35] W. Ma, C. Yang, X. Gong, K. Lee, A.J. Heeger, Thermally stable, efficient polymer solar cells with nanoscale control of the interpenetrating network morphology, Adv. Funct. Mater. 15 (2005) 1617–1622.
[36] W. Li, C. Du, F. Li, Y. Zhou, M. Fahlman, Z. Bo, F. Zhang, Benzothiadiazole-based linear and star molecules: design, synthesis, and their application in bulk heterojunction organic solar cells, Chem. Mater. 21 (2009) 5327–5334.
[37] H.-H. Liao, L.-M. Chen, Z. Xu, G. Li, Y. Yang, Highly efficient inverted polymer solar cell by low temperature annealing of Cs_2CO_3 interlayer, Appl. Phys. Lett. 92 (2008) 173303.
[38] M.T. Taschuk, M.M. Hawkeye, M.J. Brett, P. Martin (Eds.), Handbook of Deposition Technologies for Films and Coatings: Science, Applications and Technology, third ed., William Andrew Publishing (Elsevier), Oxford, United Kingdom, 2010.